ELSEVIER

Nuclear Instruments and Methods in Physics Research A 357 (1995) 363–368

NUCLEAR INSTRUMENTS & METHODS IN PHYSICS RESEARCH
Section A

Performance of a scintillating fibres semiprojective electromagnetic calorimeter

M. Bertino, C. Bini, G. De Zorzi *, G. Diambrini Palazzi, G. Di Cosimo, A. Di Domenico, F. Garufi, P. Gauzzi, D. Zanello

Dipartimento di Fisica, Universita' "La Sapienza", Roma, Italy
INFN Sezione di Roma, Roma, Italy

Received 19 July 1994

Abstract

A highly segmented scintillating fibres/lead electromagnetic calorimeter has been tested. Each calorimeter module has semiprojective geometry and is shaped as a wedge with an angle of (0.82)°. The fibres are however parallel to the wedge axis and the two small lateral regions are not fibre-instrumented. This simple and cheap approach to a projective geometry allows to achieve still good energy and space resolution. Results with electrons in the range 10–100 GeV are presented.

1. Introduction

Future experiments in high energy physics will make use of electromagnetic calorimeters for energy measurement and possibly for impact point determination. Sampling calorimeters made of scintillating fibres and lead could represent a good choice due to their fast response, easy construction and low cost. A remarkable effort has been done in the last years in this field (e.g. see Ref. [1]).

We have studied a lead-scintillating fibres segmented electromagnetic calorimeter with a semiprojective geometry. The modules have the shape of a truncated pyramid, in such a way that the sides are pointing towards an axis at a distance of 1.43 m. Fig. 1 shows the geometry of a module.

The main feature of this calorimeter is that the fibres fill only the parallelepiped part of a module, so that the two small lateral regions are not fibre-instrumented. The purpose of our test has been to verify how much the calorimeter performance, in terms of energy and space resolution, is affected by the loss of energy deposited in the wedge-shaped regions, which are not sampled.

2. The calorimeter

The calorimeter modules are built with a fusion technique. A heavy alloy with low temperature melting point encloses an array of thin stainless steel tubes, which contain 1 mm diameter Kuraray SCSF81 blue scintillating fibres.

The volume ratio fibres : alloy is 1 : 3.17, averaging on the whole module volume. The average radiation length is evaluated to be 1.0 cm and the Moliere radius 2.3 cm.

The calorimeter is segmented in 25 modules, 35 cm long, of 20.5×20.5 mm^2 (front) and 25.5×20.5 mm^2 (back) cross area, in such a way that the entrance face of the calorimeter approximates a portion of a 1.43 m radius cylindrical surface.

Each fibre bundle is glued to a light guide of squared section, which is optically connected to a photomultiplier via a yellow optical filter [2].

The main features of the calorimeter are summarized in Table 1.

3. Beam test and results

The test was performed at the CERN-SPS on the X5 beam. The calorimeter was placed on a platform movable with respect to the electron beam both in the horizontal and vertical directions. A telescope of two wire chambers in front of the calorimeter was used to measure the electron impact point, with a space accuracy (rms) of about 0.2 mm. The calorimeter was operated with a tilt angle of 2.5° in both horizontal and vertical directions, to avoid the well known channeling effect of the impinging electrons. Some run was also carried on with a horizontal tilt angle of 5°.

3.1. Energy resolution

Fig. 2 shows the detected energy as a function of the electron impact position for three calorimeter modules

* Corresponding author.

0168-9002/95/$09.50
SSDI 0168-9002(94)01530-9

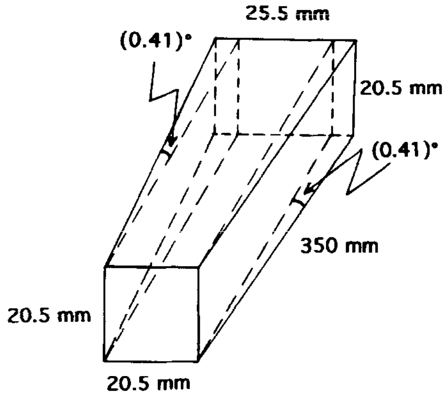

Fig. 1. Schematic view of a semiprojective module. The two lateral wedge-shaped regions with (0.41)° angular aperture are not filled with scintillating fibres.

along horizontal and vertical directions, at an electron energy of 50 GeV [1]. In the x-coordinate there is a systematic difference of about 20% between the measurement of the energy at the centre and the border of the modules, but as the impact point is measured by the calorimeter itself (see Section 3.2) a correction can be applied to the detected energy.

The calorimeter response turns out to be linear within 2% in the explored energy range 10–100 GeV, as shown in Fig. 3. The linearity does not depend on the electron impact position on the module.

The energy resolution σ/E is a linear function of $1/\sqrt{(E(\text{GeV}))}$, but there is some dependence on the impact position: $\sigma/E = (13.9 \pm 0.9)\%/\sqrt{(E(\text{GeV}))} + (1.4 \pm 0.2)\%$, at the module centre; $\sigma/E = (11.0 \pm 1.8)\%/\sqrt{(E(\text{GeV}))} + (0.6 \pm 0.4)\%$, at the middle of the module x-border; $\sigma/E = (14.0 \pm 1.8)\%/\sqrt{(E(\text{GeV}))} + (2.0 \pm 0.5)\%$, at the middle of the module y-border.

The x-border corresponds to an electron impinging between two modules, where only a fraction of the em. shower energy is sampled because the fibres are missing in the wedge-shaped volume. The y-border corresponds to the separation between two modules with full energy sampling. These results are shown in Fig. 4.

The energy resolution of this calorimeter is in agreement with the typical performance of a "spaghetti calorimeter" [1,2]. In our calorimeter the volume ratio fibres : absorber (1 : 3.17) is larger than the value 1 : 4 chosen to make the calorimeter compensating [1], but smaller than the value range 1 : 2 to 1 : 1, chosen to optimize the energy resolution [3,4].

The present result is also comparable to the performance of the semiprojective [5] and fully projective [6] "spaghetti" calorimeters having full fibre instrumented module.

Moreover it should be noticed that the energy resolution turns out to be slightly better near the non-instrumented region (i.e. at the x-border) with respect to the whole detector. Although the signal in this region is reduced by 20% with respect to the central region (see Fig. 2a), the signal fluctuation is reduced even more. We do not have a simple explanation for this phenomenon.

A set of measurements with the beam at a horizontal tilt angle of 5° (vertical tilt 2.5° as before) does not show differences both in linearity and in energy resolution with respect to those at 2.5° (see Figs. 3b and 5).

3.2. Impact point resolution

The electron "true" impact position (x, y) on the calorimeter is measured by a beam chambers telescope with an accuracy of about 0.2 mm. Horizontal and vertical scans of the beam were done, in order to explore the calorimeter response, along the x-coordinate and the y-coordinate, for the three central modules. The electron energy was 25, 50, and 100 GeV.

The (x, y) position is directly measured by the calorimeter by the energy deposited in the modules surrounding the em shower vertex. This can be done by a simple "centre of gravity" algorithm, but, as usual for segmented detectors, a better impact point determination can be achieved by more sophisticated algorithms.

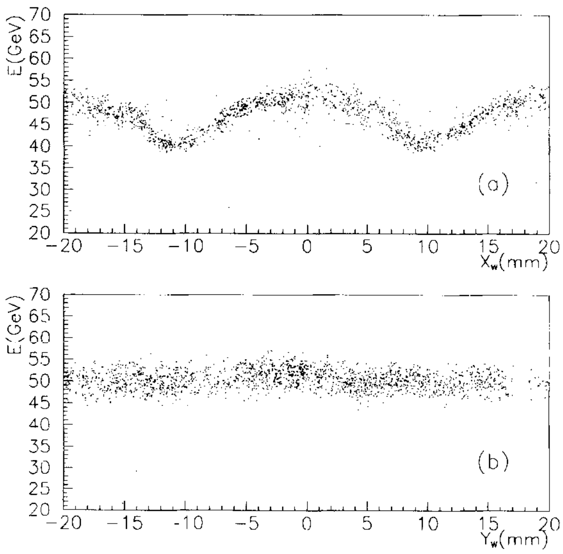

Fig. 2. The calorimeter response uniformity in the horizontal and vertical directions. Energy detected by the calorimeter as a function of the x and y impact coordinates of 50 GeV electrons. A beam scan is performed from the centre of a module (−20 cm) through a second module, up to the centre of a third module (20 cm). Two dips are seen in the horizontal scan (a), corresponding to the two non-instrumented wedge-shaped regions.

[1] This scan, as well as all other scans performed in this work, are done integrating over 5 mm in the orthogonal direction.

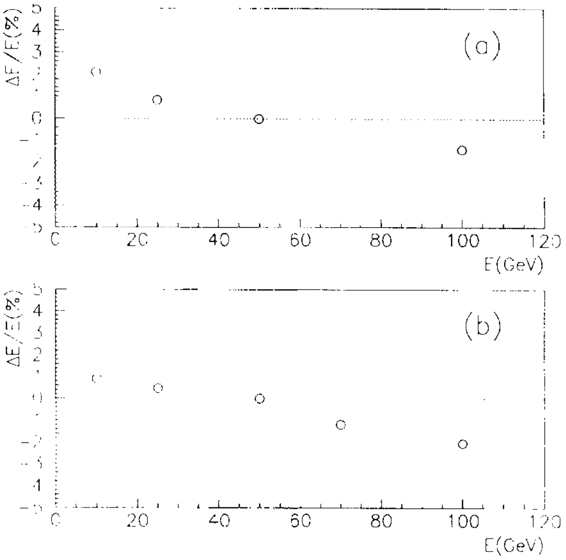

Fig. 3. Percentage non-linearity versus energy from 10 to 100 GeV. (a) The horizontal and the vertical tilt angles are 2.5°; (b) the horizontal tilt angle is 5°.

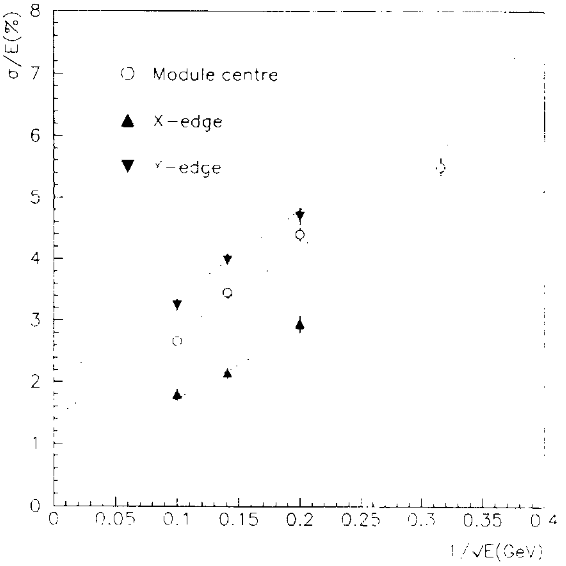

Fig. 4. Energy resolution as a function of $1/\sqrt{(E(\mathrm{GeV}))}$. The electron beam hits the module centre (circles), the x-border (upward triangles), and the y-border (downward triangles). The horizontal and the vertical tilt angles are 2.5°.

We have applied to our data two algorithms [2,7], and we found that the best method is obtained parametrizing the dependence of the "centre of gravity" coordinate on the "true" coordinate with the following formula [7]:

$$x_g = a + b \arctan[c(x_w + d)], \qquad (1)$$

In Eq. (1): x_w is the x-coordinate measured with the chambers; x_g is the x-coordinate measured with the calorimeter utilizing the simple "centre of gravity" algorithm; a, b, c, and d are four parameters which are determined by fitting the experimental points (x_w, x_g) with the function (1).

The same formula holds for the y-coordinate.

Fig. 6a shows the x_g-coordinate versus the x_w-coordinate for 50 GeV electrons detected in the three central modules: the waving behaviour is typical of any modular calorimeter.

Fig. 6b shows the same data with the fit of Eq. (1) superimposed. The fit is carried on from a module centre to the adjacent module centre. (A very small discontinuity, intrinsic of this method, is seen at $x_w = 0$, but does not affect the result).

The values of the four fitted parameters do not depend on the electron energy in our energy interval.

Concerning the y-coordinate the data and the corresponding fit are shown, at 50 GeV, in Fig. 7.

For the y-coordinate the values of the parameters are slightly different, which is not surprising due to the different physical configuration along the x and y axes.

Table 1
Calorimeter's main features

Scintillating fibres	Kuraray SCSF81, 1 mm diameter
Absorber alloy (% in weight)	AF17 (52.5% Bi, 32% Pb, 15.5% Sn)
Volume ratio fibres : absorber	1 : 3.17
Average density	7.1 g/cm^3
Average radiation length	1.0 cm
Average Moliere radius	2.3 cm
Read-out PMT	XP1911
PMT photocathode diameter	14 mm
Optical filter	Kodak Wratten No. 8
Total number of read-out channels	25
Module cross area (horizontal × vertical)	20.5 × 20.5 mm^2 (front) 25.5 × 20.5 mm^2 (back)
Number of fibres per module	144
Calorimeter total cross area	10 × 10 cm^2 (front)
Calorimeter total length	35 cm

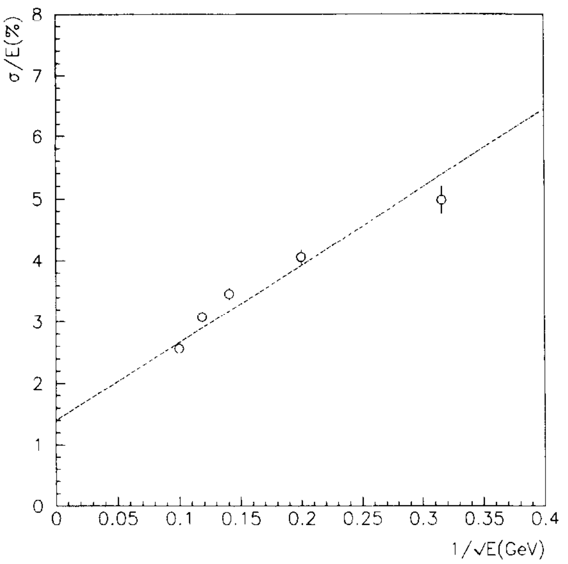

Fig. 5. Same plot as in Fig. 4, but the horizontal tilt angle is 5°. The beam hits the module centre. The linear fit yields: $\sigma/E = (12.6 \pm 0.9)\%/\sqrt{(E(\mathrm{GeV}))} + (1.4 \pm 0.2)\%$.

The parametrization (1) can be inverted as follows:

$$x_c = -d + (1/c)\tan\left[(x_g - a)/b\right] \quad (2)$$

and applied event by event in order to obtain an unbiased x_c coordinate from x_g.

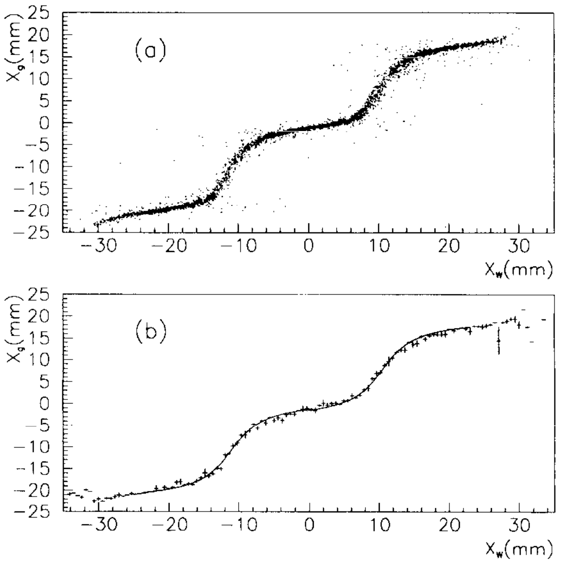

Fig. 6. (a) Comparison between the x-coordinate measured by the beam chambers, and the same coordinate reconstructed by the calorimeter with a simple "centre of gravity" algorithm. The 50 GeV electron beam scans 3 calorimeter modules, i.e., from −30 cm to 30 cm. (b) The same result is shown with superimposed the fit of Eq. (1).

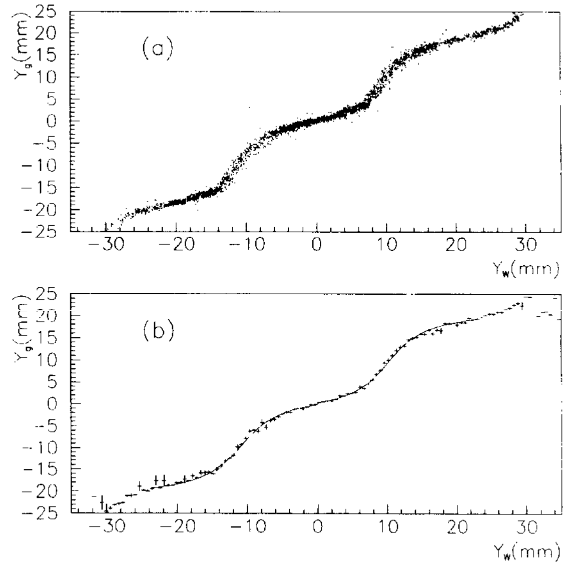

Fig. 7. (a) Same plot as in Fig. 6a, for the y-coordinate. (b) Same plot as in Fig. 6b, for the y-coordinate.

The waving behaviour in both horizontal and vertical coordinates is clearly reduced to an almost straight line by applying Eq. (2). Fig. 8 shows $x_c(y_c)$ versus $x_w(y_w)$ at 50 GeV. A small residual waving is still present, but it does not deteriorate the space resolution which is basically determined by the width of the (x_w, x_c) distribution, and

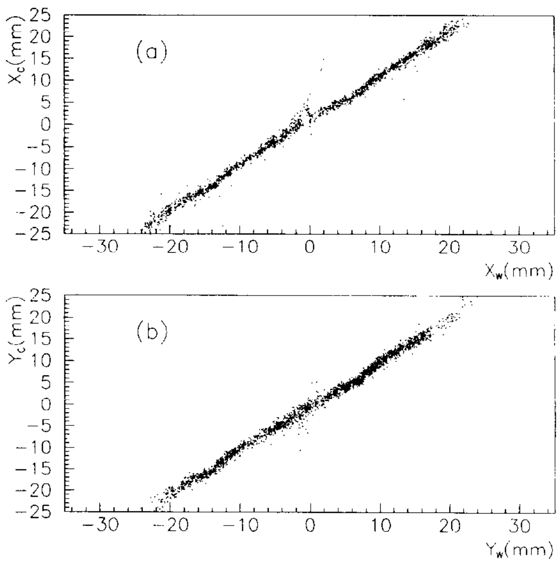

Fig. 8. (a) Scatter plot for 50 GeV electrons, showing the x-coordinate determined by the calorimeter with the algorithm of Eq. (2) versus the x-coordinate measured by the beam chambers. The centre of a module is at −20, 0, and 20 cm respectively. (b) Same plot for the y-coordinate.

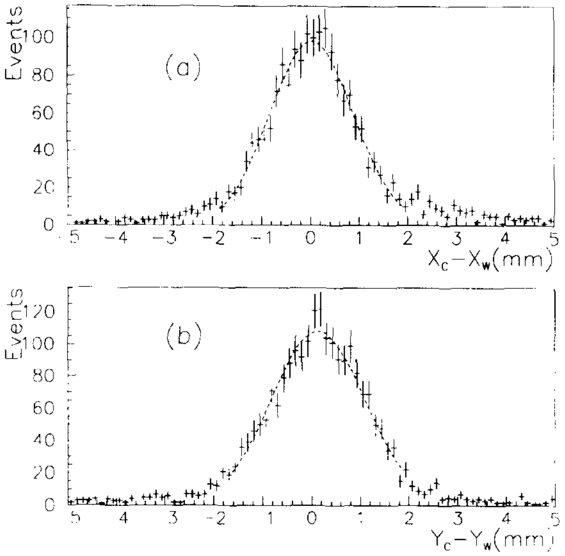

Fig. 9. (a) Distribution of the difference between the calorimeter reconstructed abscissa (see Eq. (2)) and the "true" one at 50 GeV. Fitting a Gaussian function one finds $\sigma_x = 0.87$ mm. (b) Same plot for the y-coordinate; the Gaussian fit gives $\sigma_y = 0.94$ mm.

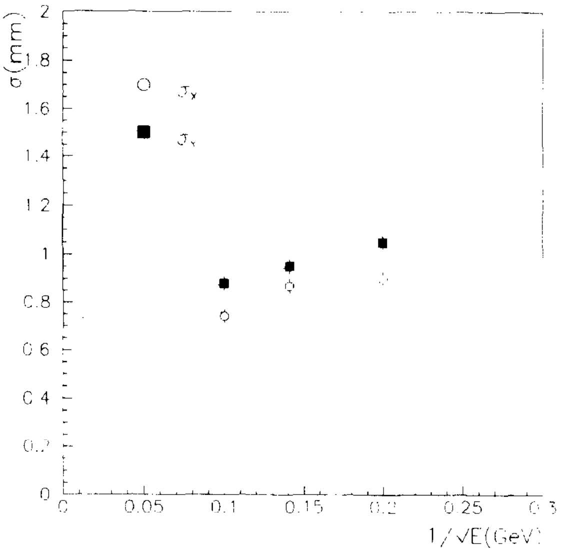

Fig. 11. Impact point resolution of the electron shower as a function of the electron energy for the horizontal (circles) and the vertical (squares) coordinate respectively. The linear fit in $1/\sqrt{(E(\text{GeV}))}$ gives the result quoted in Section 3.2.

(y_w, y_c) distribution, for the horizontal and the vertical coordinate respectively.

An example of impact points distribution as a function of the difference ($x_w - x_c$) and ($y_w - y_c$), is given in Fig. 9 at 50 GeV. The impact point resolution turns out to be slightly dependent on the impact position, as shown in Fig. 10 at 50 GeV for both coordinates.

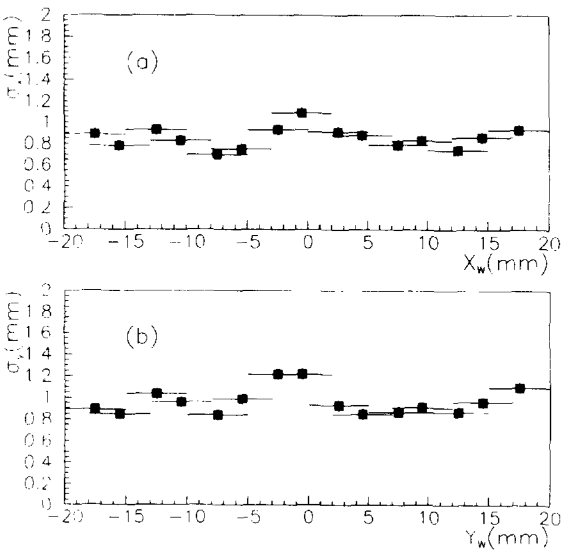

Fig. 10. Impact position resolution in x-coordinate (a), and in y-coordinate (b), as a function of the impact position x and y respectively. The module centre is at about 0 cm, and its edges at −10 cm and 10 cm. The electron energy is 50 GeV.

After all corrections the space resolution is a linear function of $1/\sqrt{(E(\text{GeV}))}$:

$$\sigma_x = (1.8 \pm 0.2)\ \text{mm}/\sqrt{(E(\text{GeV}))} + (0.6 \pm 0.1)\ \text{mm},$$

$$\sigma_y = (1.7 \pm 0.2)\ \text{mm}/\sqrt{(E(\text{GeV}))} + (0.7 \pm 0.1)\ \text{mm}.$$

This result is obtained by averaging σ over the full module size and is plotted in Fig. 11.

It is worth noting that the resolution is the same in both x and y coordinates. The different energy sampling at the two module borders in the horizontal coordinate does not affect the impact point reconstruction accuracy of this calorimeter.

The present result should be compared with the resolution obtained with highly segmented [2] and less segmented calorimeters [1,3], and furthermore having different fibres : lead volume ratio.
This comparison shows that, as expected, the statistical term is dominated by the fibres : lead ratio, while the constant term is determined by the module size.

4. Conclusions

A simple approach to the design of a segmented semiprojective em calorimeter has been carried out. This detector, made of small cross area (20.5 × 20.5 mm^2) modules, approximates a cylindrical surface of 1.43 m radius.

The main feature of this calorimeter is that the wedge-shaped lateral region, at both the sides of a module, is not filled with fibres. This considerably simplifies the construction.

The energy and the space resolution have been measured on an electron beam in an energy range from 10 to 100 GeV.

Our results show that both these features are uniform over the whole calorimeter, i.e. no worsening effect is found when the electron hits the wedge-shaped regions. The energy resolution compares with the common values of the so called spaghetti calorimeters: $\sigma/E \cong 14.0\%/\sqrt{(E(\mathrm{GeV}))} + 1.5\%$.
The space resolution, in both the coordinates, is as good as that obtained with highly segmented, but non-projective, fibres/lead calorimeters: $\sigma \cong 1.7\ \mathrm{mm}/\sqrt{(E(\mathrm{GeV}))} + 0.6$ mm.

Acknowledgements

We warmly thank R. De Salvo for many discussions and for helping us in the preparation of the test. We are grateful to L. Gatignon for his constant help during our test at the CERN-SPS beam.

References

[1] R. Wigmans, Nucl. Instr. and Meth. A 315 (1992) 299.
[2] A. Asmone et al., Nucl. Instr. and Meth. A 326 (1993) 477.
[3] S. Dagoret et al., CERN-PPE/93-147 (1993).
[4] D.W. Herzog et al., Nucl. Instr. and Meth. A 294 (1990) 446.
[5] B. Bencheikh et al., Nucl. Instr. and Meth. A 315 (1992) 354.
[6] J. Badier et al., Nucl. Instr. and Meth. A 337 (1994) 326.
[7] D. Acosta et al., Nucl. Instr. and Meth. A 305 (1991) 55.